Transport properties of the quasi-one-dimensional barium ruthenates

Y. Klein* and I. Terasaki
Department of Applied Physics, Waseda University, 3-4-1 Ohkubo, Shinjuku-ku, Tokyo 169-8555, Japan
(Received 19 June 2007; published 3 October 2007)

We measured the resistivity, thermoelectric power, and Hall coefficient of polycrystalline samples of $4H$-$Ba_{0.8}Sr_{0.2}RuO_3$ and $9R$-$BaRu_{1-x}Rh_xO_3$ ($0 \leqslant x \leqslant 0.35$) with a quasi-one-dimensional crystallographic structure made of corner- and face-shared RuO_6 octahedrons in different proportions. The magnitude of the thermoelectric power is as small as that of metals, but the sign changes from positive to negative with decreasing temperature. In contrast, the Hall coefficient is positive in the range of 4.2–300 K, and its increase at low temperatures reflects a pseudogap opening in the hole band. A simple two-carrier model is used as a qualitative explanation for the transport properties.

DOI: 10.1103/PhysRevB.76.165105 PACS number(s): 72.90.+y, 72.15.Jf

I. INTRODUCTION

Ruthenium oxides have been intensively investigated for their intriguing properties. This is well illustrated by the unconventional superconductivity in Sr_2RuO_4 with likely p-wave symmetry.[1] $CaRuO_3$ and $SrRuO_3$ with an orthorhombic perovskite structure show similar metallic resistivities with $\rho_{300\ K} \approx 200\ \mu\Omega$ cm for single crystals,[2] but the former is a Curie-Weiss paramagnet situated on the verge of a magnetic state,[3] while the latter is an itinerant ferromagnet below $T_C \approx 163$ K.[4] Recently, their thermoelectric powers (S) were measured up to high temperature, and they show T-independent values of 34 μV/K above 300 K.[5] This is a fairly high value if one considers the good conductivity of these oxides.

$BaRuO_3$ has a different crystal structure from $CaRuO_3$ and $SrRuO_3$, and crystallizes in the $4H$ hexagonal or $9R$ rhombohedral phases.[6,7] Figure 1 shows a schematic structure of these polytypes. In the $9R$ phase ($R\bar{3}m$ group), the Ru_3O_{12} strings constituted of three RuO_6 octahedra sharing faces along the c axis are connected together at the corners, resulting in a zigzag chain structure. In the $4H$ phase ($P6_3/mmc$ group), the partial Ru_2O_9 strings are constituted of two face-shared RuO_6 octahedra. The Ru-Ru bond between the face-shared octahedra is approximately 2.53 Å for both compounds, less than the shortest distance in Ru metal (2.65 Å), which favors a direct metallic interaction along the c axis. In contrast, the Ru-Ru interactions between the corner-shared octahedra are negligible, as seen in $CaRuO_3$ and $SrRuO_3$, in which the Ru t_{2g} electrons interact through the $2p$ orbitals of the intermediate oxygen ion. Different Ru-O-Ru bond angles for $CaRuO_3$ (150°), $SrRuO_3$ (162°), and $BaRuO_3$ (180° for corner-shared octahedra) can also induce different physical properties. Even if the crystallographic structures of these compounds show clear differences, the gross features of the calculated density of states (DOS) are very similar in the vicinity of the Fermi level (E_F), with a relatively high value of 3.2 states f.u.$^{-1}$ eV^{-1} in the case of $BaRuO_3$.[8] As a consequence, similar transport properties can be expected in $ARuO_3$ (A=Ca, Sr, or Ba).

The barium ruthenates show metallicity as good as $CaRuO_3$ and $SrRuO_3$. At 300 K, the resistivity of the $4H$ compound is approximately 400 $\mu\Omega$ cm in the ab plane and 550 $\mu\Omega$ cm along the c direction.[9] For the $9R$ compound, ρ_{ab} and ρ_c are evaluated at 350 and 160 $\mu\Omega$ cm, respectively.[9] However, the temperature dependences are different at low temperatures. While the resistivity of $4H$-$BaRuO_3$ stays metallic down to very low temperatures, $9R$-$BaRuO_3$ shows an upturn below 100 K. From optical conductivity measurements, the opening of a pseudogap has been suggested by Lee *et al.* for both compounds.[10,11]

We report the thermoelectric power and Hall coefficient (R_H) of $4H$-$Ba_{0.8}Sr_{0.2}RuO_3$ and $9R$-$BaRu_{1-x}Rh_xO_3$ ($0 \leqslant x \leqslant 0.35$) from 4.2 to 300 K. In high temperature superconductors, these quantities have been extensively studied because they can probe the pseudogap and its effects on the electronic properties.[12,13] From the transport properties, we confirm the formation of a pseudogap in the $4H$ and $9R$ compounds. The latter is found to be very robust against the Ru for Rh substitution. The physical properties of Ba-based ruthenates and that of Ca- and Sr-based ruthenates are compared.

II. EXPERIMENT

Polycrystalline samples of $Ba_{0.8}Sr_{0.2}RuO_3$ and $BaRu_{1-x}Rh_xO_3$ (x=0, 0.05, 0.1, 0.15, 0.25, and 0.35) were prepared through a solid state reaction. A stoichiometric amount of $BaCO_3$, RuO_2, $SrCO_3$, and Rh_2O_3 was mixed and calcined at 1000 °C for 12 h in air. The product was finely ground, pressed into a pellet, and sintered at 1100 °C for 24 h in air.

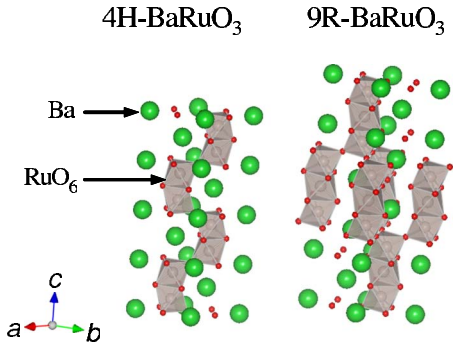

FIG. 1. (Color online) Crystal structure of $4H$ (left) and $9R$ (right) $BaRuO_3$.

The x-ray diffraction was measured using a standard diffractometer with Cu $K\alpha$ radiation as an x-ray source in the θ-2θ scan mode. The resistivity was measured through a four-terminal method, and the thermoelectric power was measured using a steady-state technique with a typical gradient of 0.5 K/cm. The Hall coefficient (R_H) was measured from 4.2 to 300 K by using a Physical Property Measurement System from Quantum Design. To eliminate the unwanted voltage arising from the misalignment of the voltage pads, the magnetic field (H) was swept from −5 to 5 T with a typical period of 20 min at constant temperature. R_H was obtained from the slope of the Hall resistance R_{xy} given as $[R_{xy}(H)-R_{xy}(-H)]/2H$.

We note that for polycrystalline samples, the thermoelectric power and the Hall resistance are independent of the carrier diffusion at the grains boundaries,[14] and these measurements qualitatively give intrinsic data for single crystals along the most conductive direction. On the other hand, the resistivity includes some extrinsic part due to the scattering of electrons by grain boundaries.

III. RESULTS

A. X-ray diffraction

Figure 2 shows the x-ray diffraction patterns of the prepared samples. For the $Ba_{0.8}Sr_{0.2}RuO_3$ sample, all the peaks are indexed as the 4H phase. Sr (isovalent to Ba) is a good element for stabilizing this phase with the Ru valence unchanged. For the $BaRuO_3$ sample (x=0), almost all the peaks are indexed as the 9R phase, but two tiny ones corresponding to the 4H phase are also present (as marked with gray circles), which disappear for $x \geqslant 0.05$. This indicates that Rh is a good element for stabilizing the 9R phase.

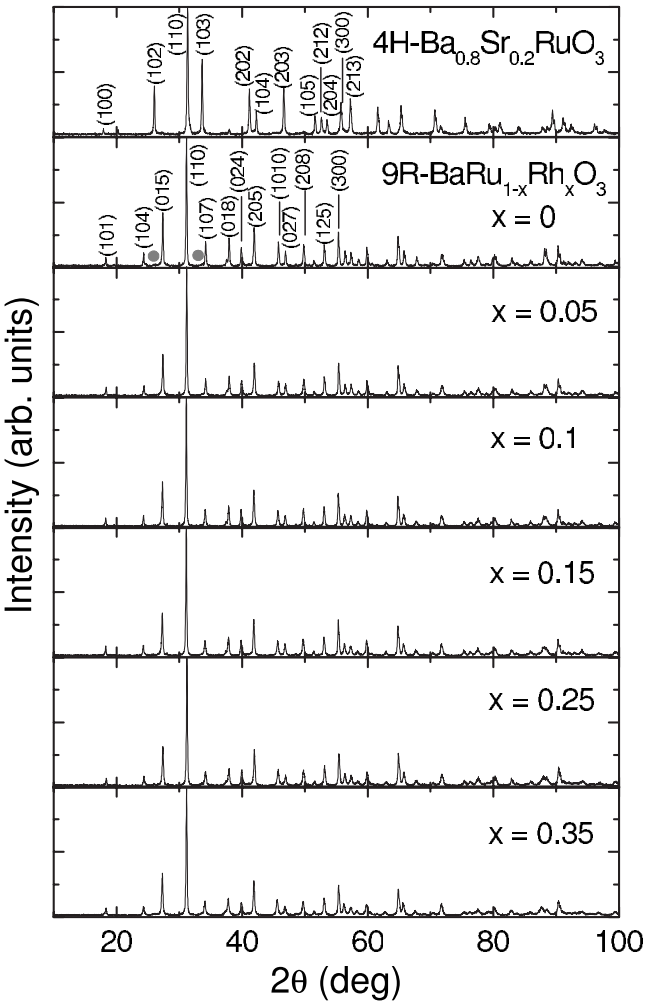

FIG. 2. X-ray diffraction patterns of the polycrystalline samples of $Ba_{0.8}Sr_{0.2}RuO_3$ and $BaRu_{1-x}Rh_xO_3$. The Cu $K\alpha$ is used as an x-ray source.

B. 4H-$Ba_{0.8}Sr_{0.2}RuO_3$ and 9R-$BaRuO_3$ properties

Figure 3(a) shows the temperature dependence of the resistivity of 4H-$Ba_{0.8}Sr_{0.2}RuO_3$ and 9R-$BaRuO_3$ samples. At room temperature, the value of the resistivity of the latter is of the order of 8 mΩ cm and $\rho(T)$ shows a metalliclike behavior that persists down to 90 K. When the sample is cooled to lower temperatures, the resistivity increases, reaching a value of 12.5 mΩ cm at 4.2 K. In the case of 4H-$Ba_{0.8}Sr_{0.2}RuO_3$, the resistivity is metallic from 300 K down to 4.2 K, with a residual resistivity evaluated to be 0.9 mΩ cm. Our data are in good accordance with the previous study of single crystals,[9] which means that our measurement shows the resistivity of pure 9R and 4H phases, and that the secondary 4H phase and the Sr doping have little influence.

Figure 3(b) shows the temperature dependence of the thermoelectric power for 4H-$Ba_{0.8}Sr_{0.2}RuO_3$ and 9R-$BaRuO_3$. At room temperature, both samples show metalliclike Seebeck coefficients with positive values of 6 and 16 μV/K, respectively. When the temperature is decreased, there is a sign change from positive to negative values at around 210 and 100 K, and a minimum is reached at around 80 and 35 K for the 4H and 9R phases, respectively. Then, the thermoelectric power goes to zero. From this result, we can conclude that positive and negative carriers drive the electronic transport of Ba-based ruthenates. The lower values for the 4H phase are in accordance with better electrical conductivity. The situation in $SrRuO_3$ and $CaRuO_3$ (Refs. 5 and 15) is different since these two ruthenates show a positive Seebeck coefficient from 5 to 800 K and a constant value of S from 200 to 800 K. Thus, we can conclude that the crystallographic structure plays an important role on the thermoelectric power.

In order to better understand the role of electrons and holes, we measured the Hall coefficient [Fig. 3(c)]. Contrary to the thermoelectric power, R_H is positive from 4.2 to 300 K, which clearly demonstrates that the two types of carriers play different roles. In other words, the carrier concentrations (n and p) and/or the mobilities (μ_n and μ_p) must be very different. For both compounds, there is an increase of R_H with decreasing temperature, followed by a decrease at low temperature. The values of R_H at 200 K are 4.6×10^{-4} and 2.1×10^{-3} cm^3/C for the 4H and 9R compounds, respectively. Values of 5.2×10^{-4} and 4.2×10^{-4} cm^3/C have been reported for $SrRuO_3$ and $CaRuO_3$ single crystals, respectively.[2] For thin films of the two single

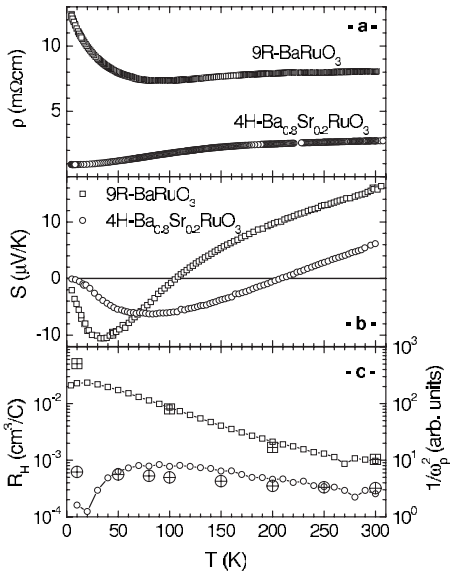

FIG. 3. (a) The resistivity ρ, (b) the thermoelectric power S, and (c) the Hall coefficient R_H (left axis, small symbols) of $4H$-$Ba_{0.8}Sr_{0.2}RuO_3$ and $9R$-$BaRuO_3$. For both samples, the Drude weight (right axis, crossed squares for $9R$-$BaRuO_3$ and crossed circles for $4H$-$Ba_{0.8}Sr_{0.2}RuO_3$) is taken from Refs. 10 and 11. In order to compare R_H with $1/\omega_p^2$, the magnitude of $1/\omega_p^2$ in (c) is properly chosen.

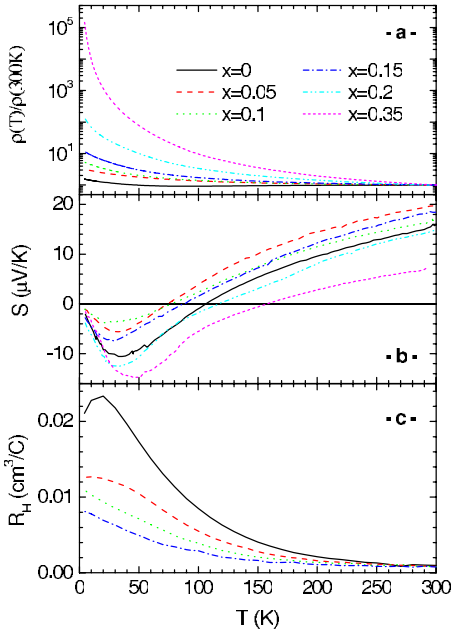

FIG. 4. (Color online) (a) The resistivity ρ, (b) the thermoelectric power S, and (c) the Hall coefficient R_H of $9R$-$BaRu_{1-x}Rh_xO_3$. Black, $x=0$; red, $x=0.05$; green, $x=0.1$; blue, $x=0.15$; cyan, $x=0.2$; and magenta, $x=0.35$.

crystals, values of 3×10^{-4} and 2.5×10^{-4} cm^3/C are found in the literature.[16] The Hall coefficient is of the same order for the ruthenates, except for $9R$-$BaRuO_3$, in which R_H is ten times larger. We should note that in contrast to the Ba-based compounds, R_H in $SrRuO_3$ and $CaRuO_3$ change the sign from positive to negative with decreasing temperature, while the thermoelectric power remains positive. These opposite situations suggest different electronic structures. The larger carrier concentration for the $4H$ phase as compared to the $9R$ phase is consistent with the lower electrical resistivity and the smaller thermoelectric power.

C. Properties of rhodium substituted ruthenates

Figure 4(a) shows the resistivity normalized at 300 K, $\rho(T)/\rho(300\ \mathrm{K})$ of the $BaRu_{1-x}Rh_xO_3$ $(0\leqslant x\leqslant 0.35)$ series. For $x\geqslant 0.05$, the metallic behavior is completely suppressed, the localization being more and more important. At 5 K, the resistivity is enhanced by approximately 5 orders of magnitude for 35% substitution. A similar localization effect is observed in the $SrRu_{1-x}Rh_xO_3$ series,[17] but, in our case, the curves cannot be fitted by a variable range hopping model nor an activation energy model.

The substitution of ruthenium for rhodium does not change dramatically the value of S at room temperature [Fig. 4(b)] except for $x=0.35$, for which S is about half of S for $x=0$. We cannot see any systematic change of the Seebeck coefficient with the rhodium concentration. The situation is similar in $SrRu_{1-x}Rh_xO_3$, in which a high content of rhodium is needed to modify the shape of $S(T)$.[17]

Contrary to the low and nonsystematic sensibility of $S(T)$ to the substitution of Ru for Rh, we observe a systematic decrease of $R_H(T)$ with the Rh content [Fig. 4(c)], particularly at low temperatures. However, in comparison with ρ, R_H shows a moderate evolution with the rhodium content, which is in agreement with the thermoelectric power data.

A Hall coefficient of 9.7×10^{-4} cm^3/C for $9R$-$BaRuO_3$ at 300 K corresponds to 0.44 holes/Ru if we neglect the electron contribution at this temperature (see the discussion below). As a consequence, if we simply suppose that Rh provides one carrier per atom, the relative variation of carriers for the $x=0.15$ sample is only 34%. This confirms that, as a semimetal, $BaRuO_3$ contains a large amount of carriers, of the order of 0.1 holes/Ru. In this context, we can understand the weak Rh dependences of the thermoelectric power and the Hall coefficient in the $BaRu_{1-x}Rh_xO_3$ series. On the other hand, the substitution strongly increases the resistivity, in particular, at low temperatures. Rh cations can act as scattering centers for electronic carriers, resulting in a strong localization.

IV. DISCUSSION

A. Pseudogap and two-carrier model

From optical conductivity measurements, Lee *et al.* have reported the plasma frequency ω_p and the scattering time τ for $9R$-$BaRuO_3$ and $4H$-$BaRuO_3$.[10,11] They analyzed these two quantities in terms of one type of carrier, but we know from our thermoelectric power measurement that electrons and holes contribute to the transport properties of Ba-based ruthenates. For a two-carrier model, the Drude weight $(\varepsilon_0\varpi_p^2/e^2)$ is proportional to the sum of the hole and electron contributions:

$$\varpi_p^2 \propto \left(\frac{p}{m_p} + \frac{n}{m_n}\right), \tag{1}$$

where m_n and m_p are the effective masses of electrons and holes, respectively. For the Hall coefficient and the electrical conductivity, we use the following expressions:

$$(\sigma_p + \sigma_n)^2 e R_H = \left(\frac{\sigma_p^2}{p} - \frac{\sigma_n^2}{n}\right), \tag{2}$$

$$\sigma = \sigma_p + \sigma_n = ne\mu_n + pe\mu_p, \tag{3}$$

where σ_p (σ_n) is the electrical conductivity for holes (electrons). We should note that the sum of the hole and electron contributions determines ω_p^2, while the difference determines R_H. For both compounds, we have plotted the quantity $1/\omega_p^2$ from Refs. 10 and 11 together with the Hall coefficient [right axis of Fig. 3(c)]. In the case of $9R$-$BaRuO_3$, one can see the good proportionality between the Hall coefficient and the Drude weight, except for low temperatures. In the case of $4H$-$BaRuO_3$, $1/\omega_p^2$ and R_H are reasonably related to each other except for low temperatures. The easiest way to understand this proportionality is to regard electrons as minority carriers with mobilities of the same order for electrons and holes, i.e., $n \ll p$ and $\mu_n \approx \mu_p$. As a consequence, we can assume ω_p^2 and $1/(eR_H)$ as direct measurements for p/m_p and p.

The Drude weight gives the sum of p and n if $m_p \sim m_n$. As a consequence, for a two-carrier compound, we cannot address the evolution of ω_p^2 by considering only optical measurements. By combining ω_p^2 with R_H, we can much more clearly discuss the decrease in the DOS near E_F. According to our work, the increase of R_H with decreasing temperature is related to the decrease of the hole concentration. Therefore, we can attribute this behavior to the opening of a pseudogap in the hole band.

The effects of the pseudogap on the resistivity are different for the two compounds. In $4H$-$BaRuO_3$, $d\rho/dT$ is positive down to 4.2 K, and in $9R$-$BaRuO_3$, $d\rho/dT$ changes its sign from positive to negative near 90 K. This difference can be ascribed to the different values of p and μ_p. The reason for the good metallic state in $4H$-$BaRuO_3$ is that a large increase of τ_p overcomes a small decrease of p at low temperatures.[11] In comparison, in $9R$-$BaRuO_3$, the decrease of p is much more dramatic to cause the semiconducting-like resistivity at low temperatures.[10]

One can see at low temperature a decrease of the Hall coefficient for both compounds, and consequently, the carrier concentration seems to increase again. However, it is more reasonable to consider the two-carrier model as follows. If we suppose the same mobilities for holes and electrons, the Hall coefficient can be simplified to the following expression:

$$neR_H = \frac{p/n - 1}{(p/n + 1)^2}. \tag{4}$$

We have plotted the right-hand term as a function of p/n in Fig. 5. Assuming that at high temperature holes are the majority carriers, we find that $R_H \to 1/ep$, as explained above.

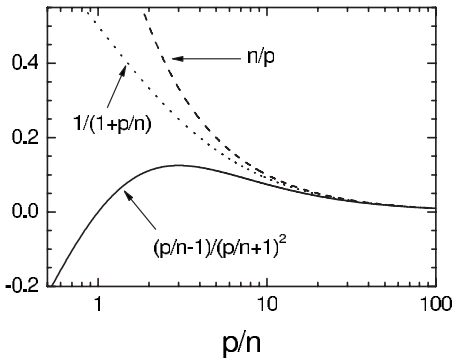

FIG. 5. $(p/n-1)/(p/n+1)^2$, $1/(p/n+1)$, and n/p calculated as a function of p/n. p and n are the carrier concentrations for the hole and electron bands, respectively.

With decreasing temperature, the pseudogap opens in the hole band to decrease p. As the holes become fewer and fewer, the numbers of holes and electrons start to be comparable and the latter plays a more important role. At a certain point, depending on the sensibility of the pseudogap to the temperature, n and p can be the same, resulting in $R_H \to 0$. We should not interpret such a small R_H as a high carrier concentration. In between the two regimes, there is a maximum that is reached for $p \sim 3n$. Assuming that n is independent of temperature, our simple model explains the experimental data qualitatively [Fig. 3(c)]. The maximum is found at 90 K for 4H-$Ba_{0.8}Sr_{0.2}RuO_3$ and at 20 K for $9R$-$BaRuO_3$.

On the same idea, we can simplify the Drude weight as

$$\frac{ne^2}{\varepsilon_0 m}\frac{1}{\varpi_p^2} = \frac{1}{p/n + 1} \tag{5}$$

In Fig. 5, we also plot the right-hand term of this expression, and we can clearly see the similar behavior between quantities (4) and (5) in the limit of high hole concentration. On the contrary, the two quantities deviate as $p/n \to 0$. The opening of the pseudogap in the hole band is responsible for a large decrease of p. As such phenomenon does not occur in the electron band, p/n can effectively decrease if the temperature is decreased. Experimentally, we can observe the deviation between R_H and $1/\omega_p^2$ at low temperatures, for the $9R$ and $4H$ compounds. Again, we show a qualitative accordance between the two-carrier model and the experimental data.

In the two-carrier model, the Seebeck coefficient is given by

$$(\sigma_p + \sigma_n)S = \sigma_p S_p - \sigma_n S_n, \tag{6}$$

where S_p and S_n are the absolute values of the thermoelectric power of holes and electrons, respectively. At high temperature, holes are the majority carriers, so we can neglect the electron contribution, and find S to be positive. If the samples are cooled, the number of holes decreases progressively, resulting in p and n values of the same order. Concomitantly, the sign of S can change from positive to negative. In order to make a more precise analysis, we need to

know S_p and S_n that depend on the shape of the DOS for the n- and p-type carriers in the vicinity of E_F.

B. Thermoelectric properties of ruthenates

The Seebeck coefficient of metallic ruthenates with the $4d^4$ configuration is very different from one composition to another one. Up to now, for $T>300$ K, T-independent values of S have been reported for $CaRuO_3$ ($S\approx 34\ \mu V/K$),[5] $SrRuO_3$ ($S\approx 34\ \mu V/K$),[5,18] and Sr_2RuO_4 ($S\approx 26-28\ \mu V/K$).[5,19] Such values are fairly high if one considers the metallic resistivity of all these compounds with $\rho_{300\ K}\approx 0.2\ m\Omega\ cm$.[20] On the other hand, S for $BaRuO_3$ in the $9R$ and $4H$ phases is as small as that for typical metals. At room temperature, we have measured low values of 16 and 6 $\mu V/K$, respectively.

A high thermoelectric power together with a high electronic contribution to the specific heat, or Sommerfeld coefficient γ, have been measured in layer cobaltites such as Na_xCoO_2,[21] $[Bi_{1.74}Sr_2O_4][CoO_2]_{1.82}$,[22] and $Ca_3Co_4O_9$.[23] It was proposed that the high thermoelectric power is linked to the strongly correlated nature of electronic carriers.[24] In particular, it was shown that this relation exists in layer cobaltites.[25] Looking for γ values of ruthenates into the literature, we find that high values of γ for $CaRuO_3$ [74–82 mJ mol^{-1}(Ru) K^{-2}],[26–28] $SrRuO_3$ [27.6–30 mJ mol^{-2}(Ru) K^{-2}],[16,27–29] and Sr_2RuO_4 [39–42 mJ mol^{-1}(Ru) K^{-2}] (Refs. 20 and 30) are reported, while a small value, 7.7 mJ mol^{-1}(Ru) K^{-2} has been measured in $9R$-$BaRuO_3$.[2] This is in accordance with the rough estimation of the effective mass in the $ARuO_3$ family (A=Ca, Sr, and Ba) that decreases in this sequence.[31] As a consequence, we believe that the corner-shared structure is responsible for the presence of electronic correlations in ruthenates, while the metal-metal bonding in the face-shared structure cancels this effect. In order to evidence the link between the thermoelectric power and the electronic correlations in ruthenates, other compounds should be studied. In particular, strongly correlated ruthenates of the Ruddlesden-Popper series, such as $Sr_3Ru_2O_7$ [$\gamma\approx 110$ mJ mol^{-1}(Ru) K^{-2}] and $Sr_4Ru_3O_{10}$ [$\gamma\approx 109$ mJ mol^{-1}(Ru) K^{-2}] with metallic in-plane resistivity,[20] can be interesting for thermoelectric conversion.

V. SUMMARY

In conclusion, we measured the resistivity, thermoelectric power, and Hall coefficient of polycrystalline samples of $4H$-$Ba_{0.8}Sr_{0.2}RuO_3$ and $9R$-$BaRu_{1-x}Rh_xO_3$ ($0\leqslant x\leqslant 0.35$). The coexistence of holes and electrons, majority and minority carriers, respectively, is in accordance with the electronic structure calculations that predict very complex Fermi surface with carrier pockets in the conduction and valence bands. The carrier concentration decreases with decreasing temperature, and is in excellent agreement with the evolution of the Drude weight deduced from optical conductivity measurement. Our experiments confirm the opening of a pseudogap in the Ba-based ruthenates that can only occur in the hole band. The decrease of the carrier number is more dramatic in $9R$-$BaRuO_3$ than in $4H$-$BaRuO_3$, which can be understood by looking at the band structure. In the $4H$ ruthenate, the pseudogap can be considered as a very partial gap because many bands cross the Fermi level. In the $9R$ ruthenates, the pseudogap is more dramatic for the physical properties because only two pockets of carriers, one for electrons and one for holes, emerge at the Fermi surface. More detailed experiments and theoretical studies have to be carried out in quasi-one-dimensional Ba-based ruthenates in order to address the origin of the pseudogap.

ACKNOWLEDGMENTS

We thank S. Shibasaki, T. Nakano, and S. Ishiwata for technical support. This work was supported by the Academic Frontier Project from MEXT.

*klein@htsc.sci.waseda.ac.jp

[1] Y. Maeno, H. Hashimoto, K. Yoshida, S. Nashizaki, T. Fujita, J. G. Bednorz, and F. Lichtenberg, Nature (London) **372**, 532 (1994).
[2] M. Shepard, S. McCall, G. Cao, and J. E. Crow, J. Appl. Phys. **81**, 4978 (1997).
[3] H. Mukuda, K. Ishida, Y. Kitaoka, K. Asayama, R. Kanno, and M. Takano, Phys. Rev. B **60**, 12279 (1999).
[4] H. Kobayashi, M. Nagata, R. Kanno, and Y. Kawamoto, Mater. Res. Bull. **29**, 1271 (1994).
[5] Y. Klein, S. Hébert, A. Maignan, V. Hardy, B. Raveau, B. Dabrowski, P. Tomes, and J. Hejtmanek, in *Solid-State Chemistry of Inorganic Materials VI*, edited by R. Seshadri, J. W. Kolis, D. B. Mitzi, and M. J. Rosseinsky (MRS Symposia Proceedings No. 988E (Materials Research Society, Warrendale, PA, 2007).
[6] P. C. Donohue, L. Katz, and R. Ward, Inorg. Chem. **4**, 306 (1964).
[7] S.-T. Hong and A. W. Sleight, J. Solid State Chem. **128**, 251 (1997).
[8] C. Felser and R. J. Cava, Phys. Rev. B **61**, 10005 (2000).
[9] J. T. Rijssenbeek, R. Jin, Yu. Zadorozhny, Y. Liu, B. Batlogg, and R. J. Cava, Phys. Rev. B **59**, 4561 (1999).
[10] Y. S. Lee, J. S. Lee, K. W. Kim, T. W. Noh, J. Yu, E. J. Choi, G. Cao, and J. E. Crow, Europhys. Lett. **55**, 280 (2001).
[11] Y. S. Lee, J. S. Lee, K. W. Kim, T. W. Noh, J. Yu, Y. Bang, M. K. Lee, and C. B. Eom, Phys. Rev. B **64**, 165109 (2001).
[12] T. Takemura, T. Kitajima, T. Sugaya, and I. Terasaki, J. Phys.: Condens. Matter **12**, 6199 (2000).
[13] R. Jin and H. R. Ott, Phys. Rev. B **57**, 13872 (1998).
[14] A. Carrington and J. R. Cooper, Physica C **219**, 119 (1994).
[15] Y. Klein, S. Hébert, A. Maignan, S. Kolesnik, T. Maxwell, and B. Dabrowski, Phys. Rev. B **73**, 052412 (2006).
[16] S. C. Gausepohl, M. Lee, K. Char, R. A. Rao, and C. B. Eom, Phys. Rev. B **52**, 3459 (1995).

[17] K. Yamaura, D. P. Young, and E. Takayama-Muromachi, Phys. Rev. B **69**, 024410 (2004).
[18] F. Fukugana and N. Tsuda, J. Phys. Soc. Jpn. **63**, 3798 (1994).
[19] H. Yoshino, K. Murata, N. Shirakawa, Y. Nishihara, Y. Maeno, and T. Fujita, J. Phys. Soc. Jpn. **65**, 1548 (1996).
[20] G. Cao, W. H. Song, Y. P. Sun, and X. N. Lin, Solid State Commun. **131**, 331 (2004).
[21] Y. Ando, N. Miyamoto, K. Segawa, T. Kawata, and I. Terasaki, Phys. Rev. B **60**, 10580 (1999).
[22] T. Yamamoto, K. Uchinokura, and I. Tsukada, Phys. Rev. B **65**, 184434 (2002).
[23] P. Limelette, V. Hardy, P. Auban-Senzier, D. Jérome, D. Flahaut, S. Hébert, R. Frésard, Ch. Simon, J. Noudem, and A. Maignan, Phys. Rev. B **71**, 233108 (2005).
[24] K. Behnia, D. Jaccard, and J. Flouquet, J. Phys.: Condens. Matter **16**, 5187 (2004).
[25] I. Terasaki, Mater. Trans. **42**, 951 (2001).
[26] V. Hardy, B. Raveau, R. Retoux, N. Barrier, and A. Maignan, Phys. Rev. B **73**, 094418 (2006).
[27] T. Kiyama, K. Yoshimura, K. Kosuge, H. Michor, and G. Hilscher, J. Phys. Soc. Jpn. **67**, 307 (1998).
[28] G. Cao, S. McCall, M. Shepard, J. E. Crow, and R. P. Guertin, Phys. Rev. B **56**, 321 (1997).
[29] P. B. Allen, H. Berger, O. Chauvet, L. Forro, T. Jarlborg, A. Junod, B. Revaz, and G. Santi, Phys. Rev. B **53**, 4393 (1996).
[30] S. Nishizaki, Y. Maeno, S. Farner, S. Ikeda, and T. Fujita, J. Phys. Soc. Jpn. **67**, 560 (1998).
[31] A. Gulino, R. G. Egdell, P. D. Battle, and S. H. Kim, Phys. Rev. B **51**, 6827 (1995).